ELSEVIER

Sedimentary Geology 110 (1997) 123–145

Sedimentary Geology

Facies and depositional environment of the Holocene evaporites in the Ras Shukeir area, Gulf of Suez, Egypt

M.A.M. Aref *, O.E.A. Attia, A.M.A. Wali

Cairo University, Faculty of Science, Geology Department, Giza, Egypt

Received 4 April 1996; accepted 24 October 1996

Abstract

The Holocene evaporite sequence in the Ras Shukeir area conformably overlies marine shell banks and cross-bedded to graded-bedded beach sands and gravels. The evaporite sequence is represented by gypsum–anhydrite layers that are interbedded with mudstone layers. Field and petrographic investigations of the evaporite deposits revealed two facies types, laminated evaporite facies (primary) and nodular to enterolithic anhydrite facies (diagenetic). The laminated evaporite facies is subdivided, from the bottom to top, into regular laminated evaporite, chevron gypsum–algal micrite laminations and wavy algal laminated evaporite. Based on their textures and fabrics, the regular and wavy laminated evaporite facies are interpreted as primary deposits in a coastal lagoon and salina environment. The chevron gypsum–algal micrite facies formed by the growth of chevron gypsum at the sediment–water interface within a shallow subtidal lagoonal environment that was characterized by extensive benthic algal mats. The nodular to enterolithic anhydrite facies is secondary and formed diagenetically within a siliciclastic supratidal sediment.

Some of the laminated evaporite facies have been diagenetically altered in a supratidal sabkha environment as evidenced by the following: (1) the partial formation of nodular evaporite instead of laminated evaporite; (2) disruption of gypsum laminations by plant roots and rootlets as well as by precipitation of lenticular gypsum on the root wall; and (3) partial dissolution of halite laminae and the formation of wavy anhydrite laminae.

Consequently, the Holocene evaporites in the Ras Shukeir area were deposited in a shallow semi-closed to closed basin that was separated from the Gulf of Suez trough. Changing sea level led to progradation of the evaporite facies from subtidal to intertidal lagoon and salina to a supratidal sabkha.

Keywords: Ras Shukeir; Gulf of Suez; Holocene evaporites; facies; depositional environment; coastal lagoons; sabkhas

1. Introduction

During Holocene time, arid conditions prevailed over Egypt as evidenced by the occurrence of numerous evaporite deposits close to the present-day shorelines. These evaporites overlie or are enclosed within Quaternary gravely hills. The Holocene evaporites were described and discussed by many authors, e.g., in the Gulf of Suez region (Taher, 1988; Abdel Wahab, 1991), in the Red Sea (Purser et al., 1987; Ahmed et al., 1993), in the Mediterranean coast (Abdallah, 1966; Adindani et al., 1975; Wali, 1993), and in the Gulf of Aqaba (Sehim, 1990; El Refaeai, 1992). Most authors describe 2–3-m-thick gypsum beds that were formed in coastal lagoons or sabkhas. The Holocene evaporites of the Ras Shukeir

* Corresponding author. E-mail: Mahmoudaref@FRCU.EUN.EG

0037-0738/97/$17.00
PII S0037-0738(96)00080-2

area, Gulf of Suez, attracted the attention of the present authors as they have a modern analog in the present-day sabkha–salina complex (Abdel Wahab, 1991). Older evaporites of Middle Miocene age occur inland of the studied Holocene evaporites (Aref et al., 1995).

The present paper deals with the geology and facies of the Holocene evaporite deposits in the Ras Shukeir area, with the aim of reconstructing their depositional environment and the diagenetic processes that affected them during deposition, burial and uplift.

2. Geologic setting

The Ras Shukeir Holocene evaporites are located on the western shoreline of the Gulf of Suez (about 3 km west of Ras Shukeir, 35 km southwest of Ras Gharib city; Fig. 1). They are separated from the sea by a 1-km-wide barrier ridge of sandy, bioclastic

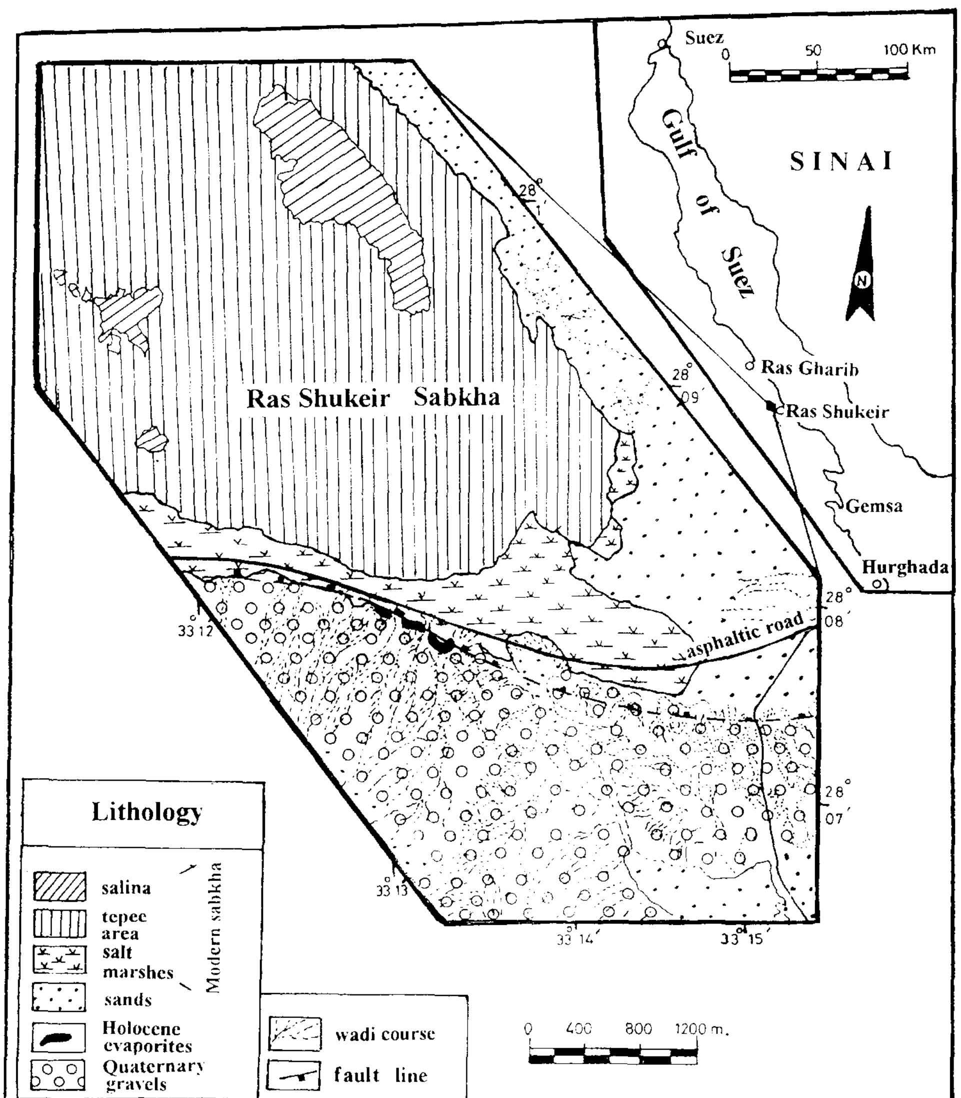

Fig. 1. Geologic map of the Ras Shukeir area.

limestones and mudstones probably of Plio–Pleistocene age (Purser et al., 1987). North of the studied evaporite rocks is a NW–SE elongated depression (Ras Shukeir sabkha) with its sandy surface 5 m below sea level (Purser, 1985). The dry sabkha plain is covered with gypsum and halite crusts that exhibit tepee structures. Near its southern extremity several small salinas occur; these have an average depth of 1 m (Purser et al., 1987; Keheila et al., 1989) and were formed along NW–SE fault lines (Wali et al., 1986).

Quaternary gravely hills, 8 m in thickness, surround the studied evaporites on the south and west. These gravely hills extend 10 km to the west, where Middle Miocene evaporites and Lower Miocene limestones and sandstones crop out (Aref et al., 1995).

The studied evaporite rocks crop out in three isolated hills separated by small wadis. The hills are located on the upthrown side of a WNW–ESE fault line, whose downthrown side is believed to be located beneath the present-day sabkha. This is evidenced by the sharp termination of the evaporite exposure toward the sabkha and the presence of 50 cm low-lying evaporite hills north of the fault line. The evaporite rocks overlie uplifted beach terraces which contain rock fragments from the surrounding Quaternary gravels (thus the evaporites are younger in age than the Quaternary gravels).

The evaporite sequence consists of gypsiferous marl at the bottom, that is overlain by laminated evaporites interbedded with cracked mudstone layers. The top part is covered with unlithified gravels that have their source in the Quaternary gravely hills.

3. Facies and depositional environment

The term 'evaporite facies' or 'evaporite sediment type' is used here in the same sense as used by Schreiber and Kinsman (1975), and Arakel (1980), respectively, and refers to a distinct sediment or sedimentary rock deposited under certain environmental conditions, irrespective of age or physiographic–stratigraphic position. Moore (1949) used the very broad term 'lithofacies' in which all evaporites were listed in a single classification, i.e. evaporite lithofacies.

In this sense, the study of the sedimentary units in the Ras Shukeir area, revealed two lithofacies types: clastic lithofacies and evaporite lithofacies. The first is subdivided into two facies types, and the second into four facies types. Each of these is described, its depositional environment interpreted, and a general depositional model is constructed.

3.1. Clastic lithofacies

Two facies constitute the clastic lithofacies: pebbly skeletal litharenite and cracked mudstone.

3.1.1. Pebbly skeletal litharenite

This is the lowermost unit of the Holocene sequence and crops out only at the base of the eastern

Fig. 2. The sedimentary sequence of the eastern hill showing low-angle cross-bedded sandstone at the bottom, overlain by laminated gypsum and anhydrite deposits and cracked mudstone layers (photo looking south).

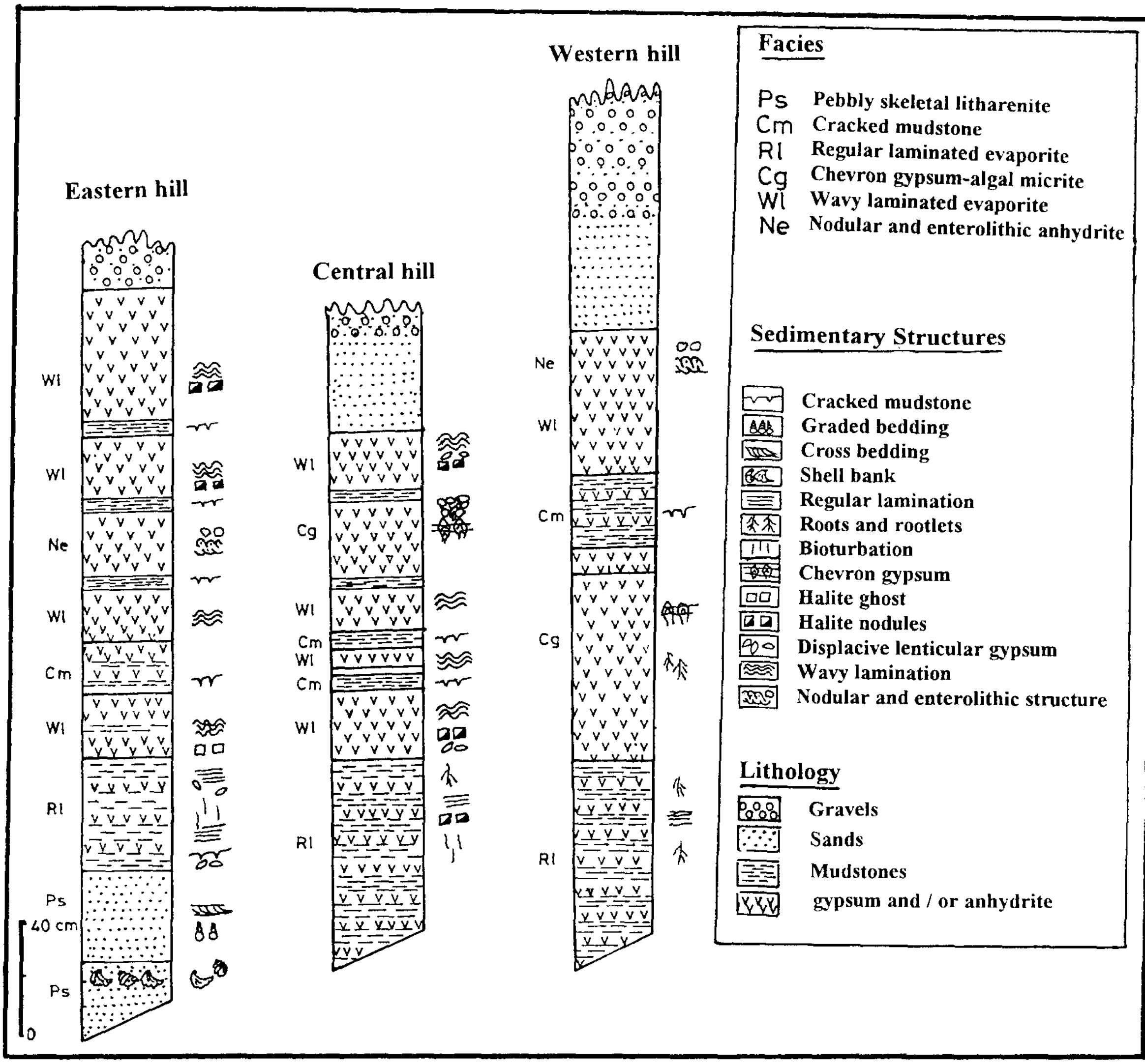

Fig. 3. Facies logs of the exposed evaporite rocks in the Ras Shukeir area.

hill (Figs. 2 and 3). It has a thickness of 50 cm that thins westward to a few centimetres. It consists of low-angle cross-bedded, medium- to coarse-grained sands and gravels that dip to the west (inland from the present-day Gulf). Each cross-bed lamina shows normal grading of the siliciclastic sediments and includes scattered shell debris. Near the bottom, a 10-cm-thick shell bank, mainly composed of pelecypod and gastropod shells (e.g., *Chama*, *Gafrium*, *Diplodonta*, *Mactra*, *Cerithium*, *Cerastoderma* and *Circe*) (G. Ismael, pers. commun., 1995), occurs. The shells are mostly in convex-upward orientation.

Under the microscope, the rock consists of mono- and polycrystalline, sub-rounded quartz grains and basement and sedimentary rock fragments derived from the nearby Quaternary gravel and the Lower to Middle Miocene limestone and evaporite rocks of the Shagar area (Aref et al., 1995). Shells and shell fragments vary in abundance, and are mainly filled with fine quartz grains (Fig. 4A).

The cement pattern differs from the base to the top part of this unit. At the base, it consists of early

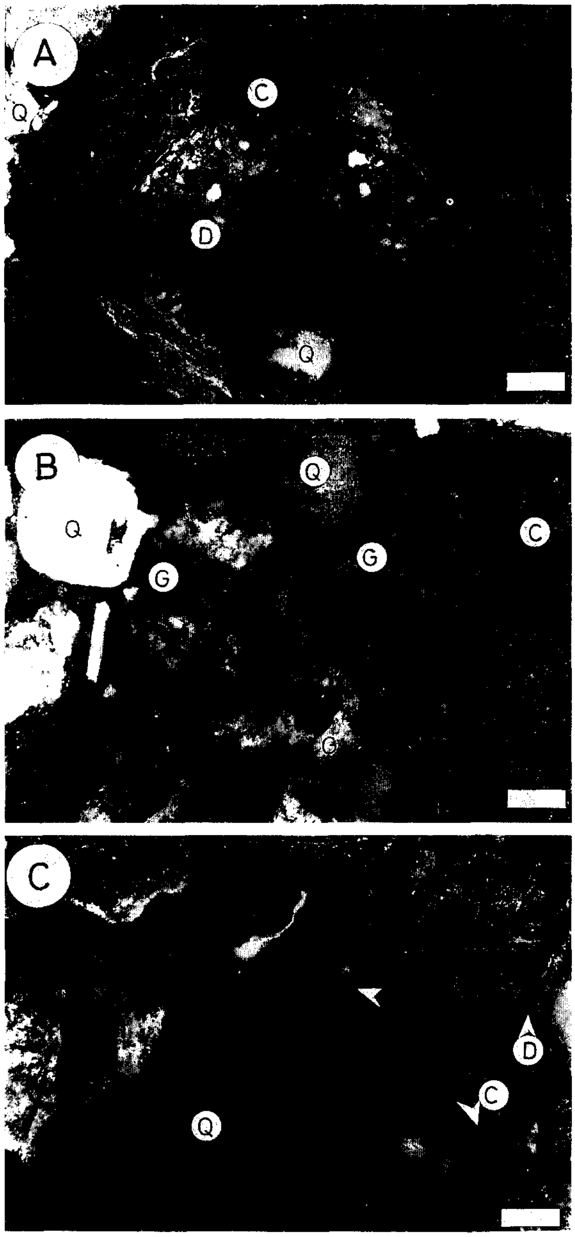

Fig. 4. Pebbly skeletal litharenite facies. (A) A calcitic shell fragment filled with detrital quartz and dolomicrite cement. Thin-section stained with Alizarin Red-S; crossed polars; bar = 250 μm. (B) A patch of poikilotopic gypsum cement enclosing detrital quartz and shell fragments. Thin-section stained with Alizarin Red-S; crossed polars; bar = 250 μm. (C) Dark calcitic micrite coating around quartz and shell fragments encrusted with dense dolomicrite and fibrous dolomite (phreatic cementation). Thin-section stained with Alizarin Red-S; crossed polars; bar = 250 μm. *C* = calcite, *D* = dolomite, *Q* = quartz, *G* = gypsum.

diagenetic dense dolomicrite that rims the sedimentary particles leaving intergranular pores, sometimes filled with patches of gypsum cement (Fig. 4B). The gypsum patches consist of single poikilotopic gypsum crystals (3000–4000 μm in size) that enclose the sedimentary particles (Fig. 4B). Similar patchworks of gypsum cement or overgrowths were recorded by Hussain and Warren (1989) from the Salt Flat playa of west Texas. They believed that the gypsum cement was diagenetically formed in a highly saline interstitial brine generated by dissolution of near-surface laminated gypsum. In the present study, gypsum was diagenetically formed as a vadose cement in the capillary zone. The sulphate ion was most probably derived by partial dissolution of the overlying laminated gypsum, as indicated by the occurrence of nodular anhydrite instead of laminated gypsum (Fig. 7C). The gypsum patches were diagenetically formed following the dense, early diagenetic isopachous dolomite cement of the phreatic zone (Fig. 4B).

Near the top of the unit the cementing material forms a rim around the sedimentary particles. This consists of a dense calcitic micrite envelop followed by dolomicrite and finally fibrous dolomite crystals that have grown into open intergranular spaces (Fig. 4C). Algae are believed to have played a role in the formation of these cements. Friedman et al. (1973) showed that algae can create a microenvironment, in which a variety of calcium carbonate fabrics and minerals can form. In such a microenvironment, Mg becomes enriched within algal mats (Gebelein and Hoffman, 1971; Monty, 1986) which in turn leads to the formation of dolomite laminae.

In the study area, algae are believed to have entrapped the sedimentary and skeletal particles, creating a microenvironment in which the entire algal layer precipitated aragonite, whereas the outer algal layer precipitated high Mg-calcite. During diagenesis, aragonite was transformed into calcite and high Mg-calcite into dolomite (Fig. 4C). The formation of these cements was controlled by algae as described by Friedman et al. (1973) from the hypersaline pools of the Red Sea. Dolomitization of the outer rim cement by the incoming high Mg-calcite solution is ruled out since all skeletal particles as well as the micrite cement are still calcitic in composition and were not affected by dolomitization.

Environment of deposition. The low-angle cross-bedded laminae in this unit, clearly point to strong, directional currents in very shallow water. They were developed mainly during storms or high water in a backshore, supratidal environment. During storms, the shell debris of marine organisms are washed from the subtidal to the supratidal environment where they get mixed with the coarser Quaternary gravels of the beach (Reineck and Singh, 1980). As the storm energy decreases, the sedimentary particles are deposited as cross-bedded laminae that slope landwards. Cementation of these beach sediments occurred in the back-shore (supratidal) environment via early diagenetic dolomite and gypsum precipitates (Patterson and Kinsman, 1982).

3.1.2. Mudstone facies

This facies shows sharp contact with the evaporite layers all over the study area (Fig. 2). Beds range in thickness from a few centimetres up to 25 cm and are typified by vertical to subvertical cracks or fractures that are partially filled with gypsum from the overlying subaqueous laminated gypsum layer (Fig. 5A). Other similar fractures, filled with clear transparent gypsum crystals or microcrystalline gypsum, were observed in the Miocene evaporites of Poland by Babel (1991). The mudstone layers also enclose transparent lenticular single gypsum crystals or chains and aggregates of lenticular gypsum crystals (Fig. 5B). The presence of displacive gypsum crystals and vertical cracks filled with gypsum is most probably related to the formation of subaqueous shrinkage cracks (Astin and Rogers, 1991) in an environment subjected to large salinity fluctuations (Plummer and Gostin, 1981).

In the study area, the subaqueous cracks were probably formed by the following processes: (1) the deposition of well flocculated clay-rich sediment in a saline water body; these clays subsequently deflocculated and contracted as fresh water periodically entered the pores and leached the salt (White, 1961); (2) the early diagenetic growth of displacive lenticular gypsum below the sediment–water interface created zones that acted as natural defects to localize crack formation and propagation (Allen, 1987); (3) subsequent loading created a dewatering shrinkage mechanism and instigated intrastratal subaqueous crack formation (Plummer and Gostin, 1981); (4) the absence of detrital materials to fill cracks and their filling by subaqueous gypsum from the overlying laminated gypsum layer confirm a subaqueous shrinkage origin for the cracks.

Environment of deposition. Each mud layer was deposited in a shallow lagoon or salina that formed when muddy floodwaters inundated the marginal evaporitic setting during a major storm flooding stage, as observed by Lowenstein and Hardie (1985) in Salina Omotepec. During flooding, the finer suspension load is carried onto the marginal-marine salina settings, where it ponds and settles together with precipitation of halite. Flooding of fresh water onto the clays leads to contraction of the clays as the halite is leached from them (White, 1961). Increase in brine salinity led to displacive growth of lenticular gypsum below the sediment–water interface. The growth of displacive lenticular gypsum controls the formation and propagation of cracks. Restriction of the salina from extra flooding leads to precipitation of subaqueous laminated gypsum that fills the open cracks.

3.2. Evaporite lithofacies

Study of the syndepositional and diagenetic features of the evaporite rocks in the Ras Shukeir area revealed the following facies (from bottom upward).

3.2.1. Regular laminated evaporite facies

This facies occurs at the bottom of the exposed evaporite hills (Fig. 3). Beds range in thickness from 40 to 65 cm. In the outcrop at the eastern hill, a 40-cm-thick bed is composed of 58 evaporite laminae interlaminated with thicker lime mud layers (Fig. 6A). Individual evaporite laminae range in thickness from 0.2 to 0.5 cm.

Under the microscope, the laminated evaporite facies consists of thin layers of networks of algal micrite alternating with granular gypsum laminae (Fig. 6B). The algal micrite networks enclose orange patches probably of organic origin. These show a web fabric (Fig. 6C) and enclose granular gypsum crystals between the unidentified algal filaments (Fig. 6B). The algal micrite layer is either disrupted (Fig. 6B), or continuous for a few centimetres. The gypsum laminae consist of clusters of granular gypsum with an average size of 400 μm, that are

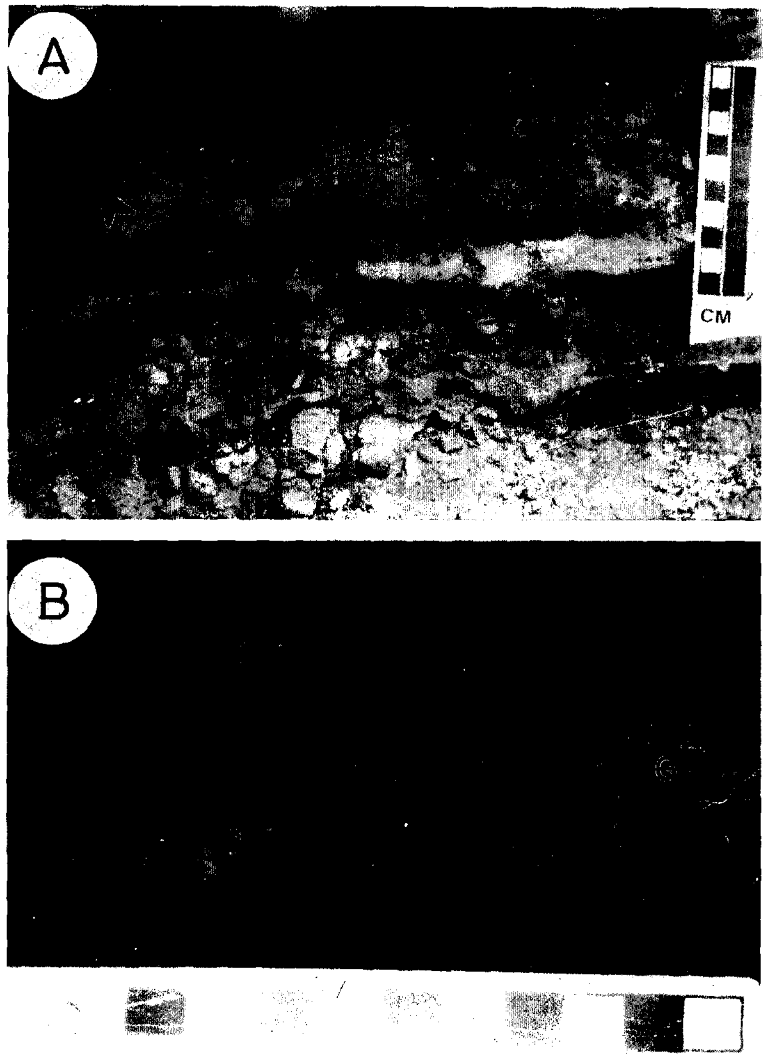

Fig. 5. Mudstone facies. (A) Cracked mudstone partially filled with gypsum (arrows) from the overlying gypsum layer. (B) A chain of lenticular aggregates of displacive gypsum crystals. G = gypsum.

tightly fused together to develop laterally continuous layers. The gypsum laminae may incorporate fine-grained micrite dispersed between the gypsum crystals (Fig. 6C). Larger gypsum crystals are observed to underlie the algal micrite laminae and may enclose disseminated micrite (Fig. 6C). This feature is similar to that recorded by Kushnir (1981) in the coastal hypersaline pools of the Red Sea. Gypsum crystals, that are surrounded with a network of algal micrite (Fig. 6B), were probably entrapped by the algal filaments.

Sometimes the normal regular laminated structure of the evaporite rock is deformed or obliterated by the occurrence of brown tubules (Fig. 7A), tree trunks (Fig. 7B), or by the occurrence of nodular anhydrite (Fig. 7C). The brown tubules lie in nearly vertical positions either at certain levels with sharp lower boundaries, or as dispersed features in the laminated evaporite facies.

Microscopically, the brown tubules are composed of coarse (400 μm) lenticular gypsum separated by algal micrite at the tubule boundary. Gypsum

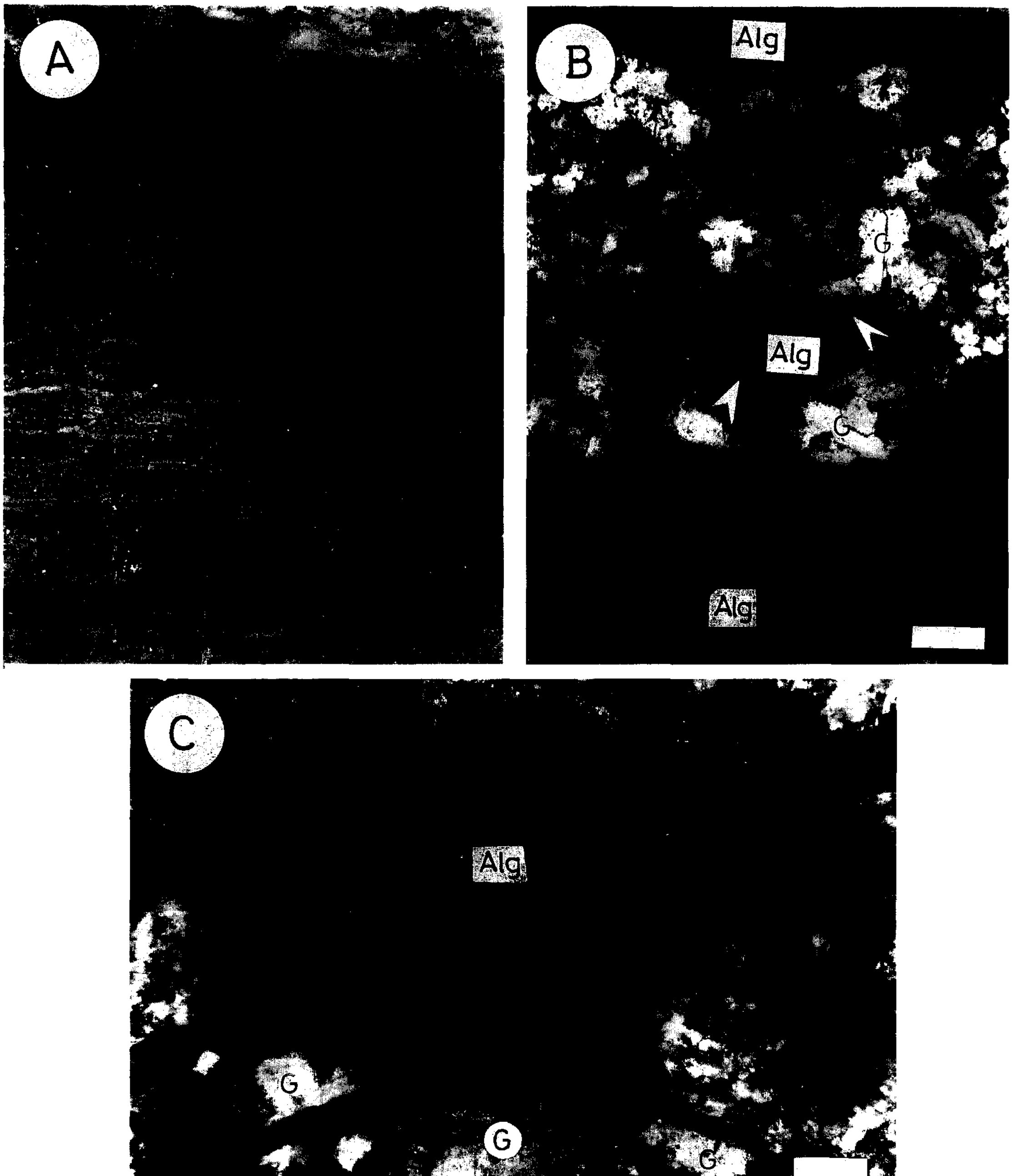

Fig. 6. Regular laminated evaporite facies. (A) Regular alternation of thin anhydrite and thicker lime mud layers. (B) Networks of algal micrite filaments that coat gypsum, overlain by granular gypsum. Crossed polars; bar = 250 μm. (C) Growth of large gypsum crystals beneath algal micrite laminae that form a web fabric. Crossed polars; bar = 250 μm. *Alg* = algal filaments, *G* = gypsum.

in the tubules decreases in size inward to form an ultimately randomly oriented mass of fine (50 μm) gypsum at the centre of the tubule (Fig. 7D). The origin of these brown tubules is not fully determined. They differ from the gypsum trees of Schreiber and Kinsman (1975) in that they lack a central tube

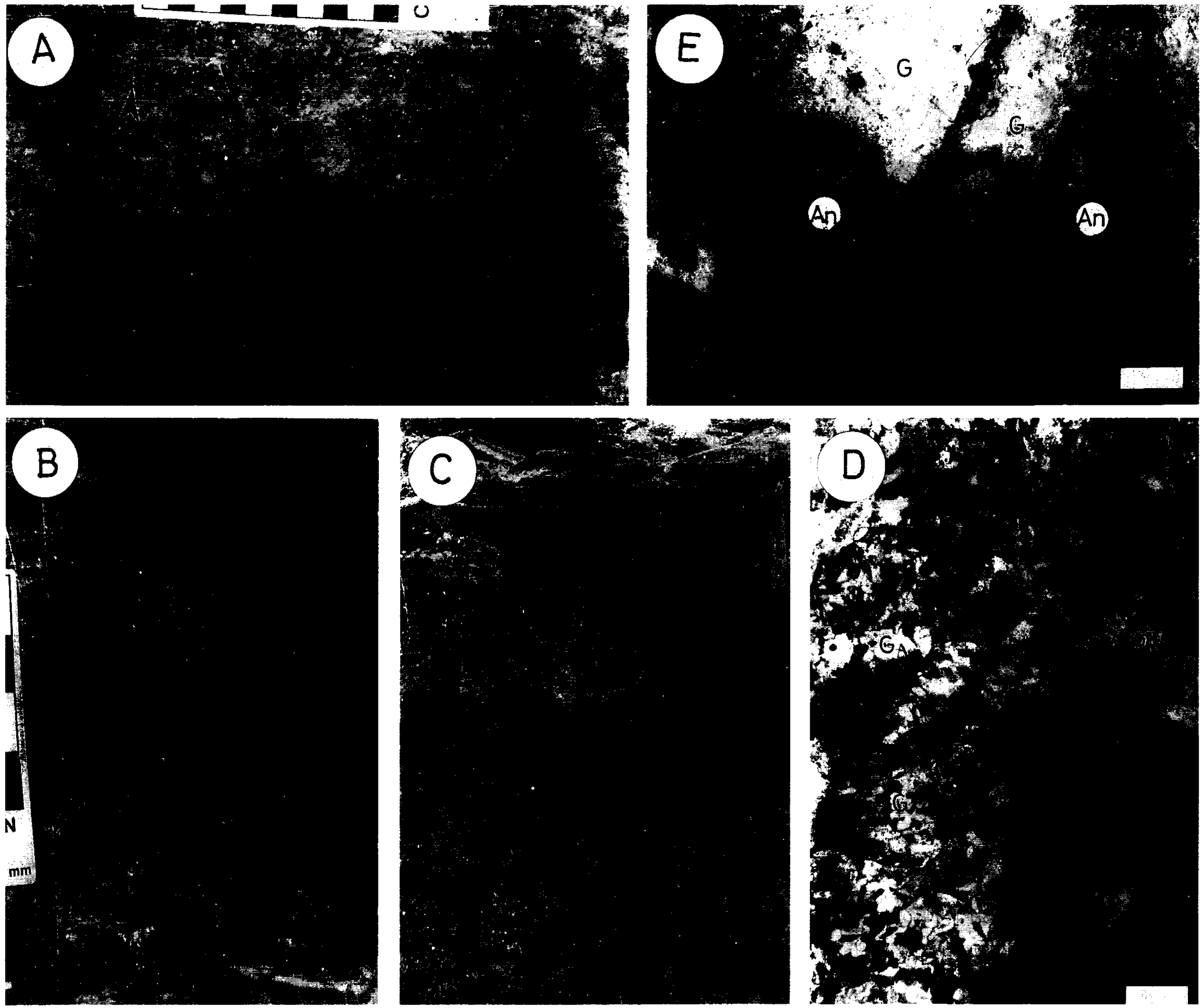

Fig. 7. Obliteration of the regular laminated structure. (A) Dark vertical tubules filled with lenticular gypsum in nodular anhydrite after an original laminated structure (arrow). (B) A tree trunk in muddy gypsum. (C) Nodular to partially dissected laminae (at top) after laminated evaporite facies. (D) Large lenticular gypsum growing at the tube boundary, grading to finer lenticular gypsum at the centre. Crossed polars. (E) Rosettes of anhydrite crystals replacing clear gypsum crystals. Crossed polars; bar = 250 μm. G = gypsum, An = anhydrite.

hollow of petrified wood, and do not show concentric arrays of crystals or root networks. The tubules can be compared with the bioturbation structures described by Bosellini and Hardie (1973) and by Salvany et al. (1994) in the Miocene evaporites of Sicily and Spain, respectively.

Irrespective of the origin of these tubules, lenticular gypsum will, most probably form in any supratidal sabkha environment that is rich in the decomposition products of continental plants (Cody and Cody, 1988). Remains of continental plants were observed in the same layer at the central hill (Fig. 7B). The lenticular gypsum crystals will grow to fill burrows and rhizoid cavities in the capillary zone when appropriate saline pore fluids of continental and marine origin mix. As the pore waters concentrate during capillary evaporation, they precipitate lenticular gypsum in the tubule hollows, which also generates intrasediment displacive crystal growth. This capillary process superimposes a new texture on the originally laminated evaporitic structure similar to that recorded by Hussain and Warren (1989), who called it 'sabkhatization' of the original subaqueous laminated evaporite facies. The overprint of the supratidal sabkha environment on the subaqueous salina setting can also be confirmed in the study area by the occurrence of a petrified tree trunk, which still shows the striations although it is now composed of powdery decayed woody material (Fig. 7B).

The second feature which led to the obliteration of the original laminated structure is the precipitation of anhydrite nodules, 1–3 cm in diameter, separated by light green marly materials (Fig. 7C), forming the classic chicken-wire or mosaic structure of Maiklem et al. (1969). Microfabrics in nodules are similar to those described by Hovorka (1992); they include mosaics of felted anhydrite with no preferred orientation and spherulitic anhydrite replacing former gypsum crystals (Fig. 7E). Gradation between the laminated gypsum to the nodular structure of anhydrite through the 40–65-cm-thick bed suggests that the nodular fabrics result from the mobility of sulphate during diagenesis (Hussain and Warren, 1989). The formation of this nodular fabric may be the result of a decrease in lagoon water level, the drying up of the bottom sediments and the introduction of low-salinity ground waters which leads to partial dissolution of the laminated gypsum. Evaporation of the resulting sulphate-rich ground waters increases the brine salinity, causing the precipitation of anhydrite nodules instead of the former laminated gypsum. This process of nodular anhydrite formation (nodulization; Peryt et al., 1993) in originally laminar evaporites has been recorded by Hussain and Warren (1989), Hovorka (1992), and Peryt et al. (1993).

Environment of deposition. Although diagenesis has partially obliterated the primary laminated structure and the internal crystal fabrics, the observed laminated structure, grain size and texture of the gypsum grains, as well as the structure of the algal micrite, are typical of sedimentation in a subtidal lagoonal environment. Similar features were recorded from the Messinian evaporite of the Mediterranean basin and have been discussed by many authors. Some of them consider periodic precipitation of gypsum during seasonal concentration of marine water (Ogniben, 1955), whereas others favour a detrital origin for the lamination (Garrison et al., 1978), and reworking of gypsum during storms (Hardie and Eugster, 1971).

Petrographic observations of the gypsum–micrite lamination in the study area indicate that the micrite (that occurs as dense aggregates with orange organic patches and as networks between and within the gypsum crystals; Fig. 6B) has originated from benthic algal plexi that flourish on the floor of a subtidal lagoonal environment (Kendall and Skipwith, 1968). As the salinity of the marine water increases, gypsum was precipitated from the water body and then settled, to be draped atop algal mats which acted like 'fly paper' (Fig. 6B). Continuous precipitation of gypsum and its reworking at the sediment surface, was also accompanied by the growth of large gypsum crystals below the sediment–brine interface. During phases of dilution of the lagoonal water, gypsum sedimentation ceased and was replaced by flourishing algal mats on the bottom sediment. Further influxes of muddy flood water into the lagoon led to deposition of lime mud over the gypsum–algal micrite lamination.

3.2.2. Chevron gypsum–algal micrite lamination facies

This facies is recorded in the central and western hills in 65–70-cm-thick beds. It is character-

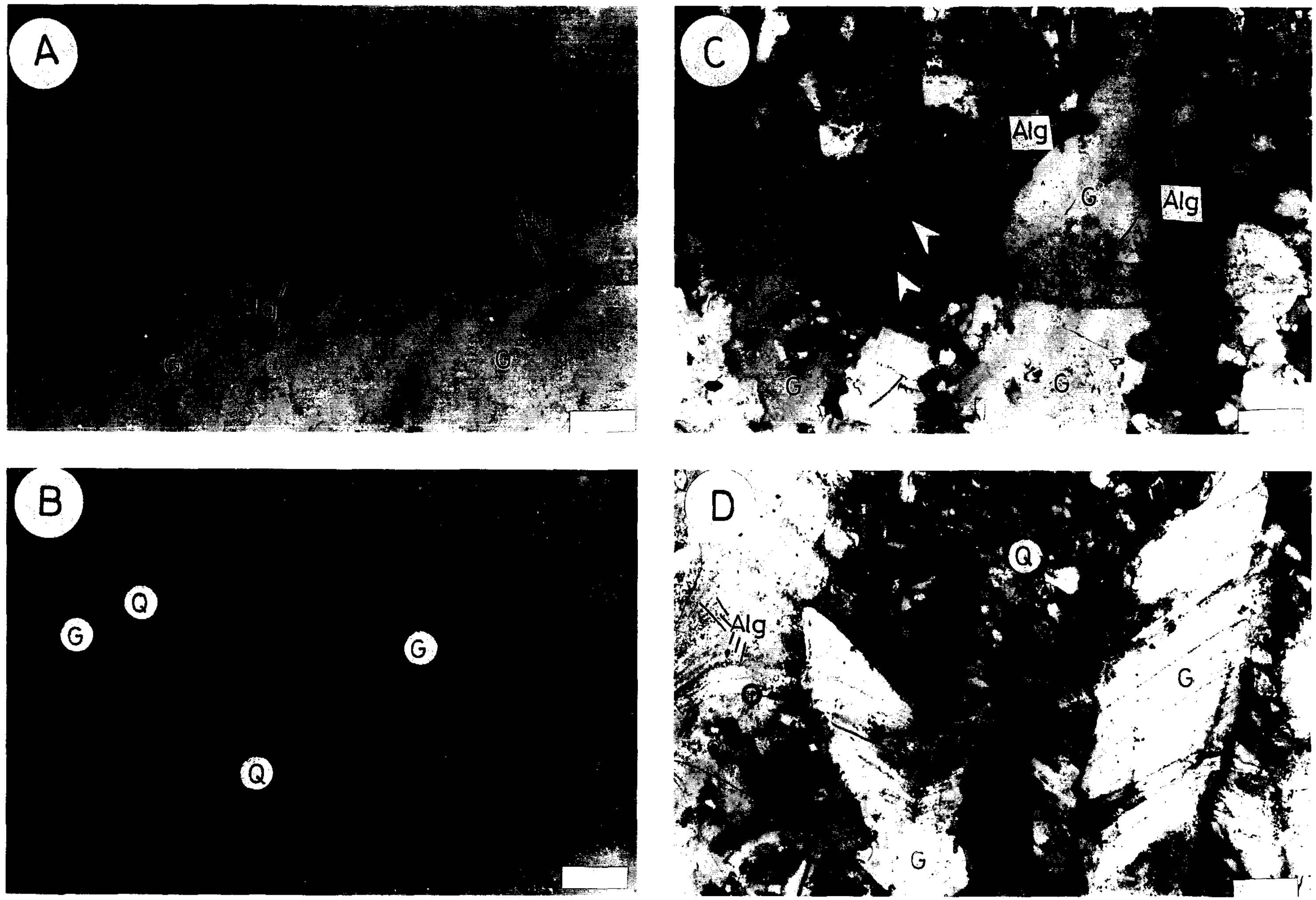

Fig. 8. Chevron gypsum–algal micrite laminated facies. (A) A layer of laterally stacked prismatic and chevron gypsum enclosing continuous and disrupted algal micrite laminae. The prismatic and chevron gypsum layer is overlain and underlain by thicker, granular gypsum layers which sometimes enclose disrupted patches of algal micrite (at top). Plane polarized light; bar = 2 mm. (B) Two layers of bottom-grown chevron gypsum crystals separated by dark clastic materials. Plane polarized light; bar = 2 mm. (C) Large chevron gypsum crystals enclosing algal micrite disrupted (at top) and continuous planar and domal (at middle). Crossed polars; bar = 250 μm. (D) Chevron gypsum enclosing algal micrite and detrital materials. The detrital materials also fill spaces between the growing chevron gypsum. Crossed polars; bar = 250 μm. *G* = gypsum, *Alg* = algal micrite, *Q* = quartz.

ized by thinly laminated, tightly to loosely packed cone-shaped prismatic and chevron gypsum crystals that are commonly confined between white, thicker gypsum laminae (Fig. 8A), or laminae of detrital particles (Fig. 8B), in the central and western hills, respectively. Individual gypsum crystals, up to 3 mm long, typically elongate in the crystallographic c-axis direction and aligned subperpendicular to the bedding (Fig. 8A), are similar to those recorded by Arakel (1980) and Rouchy and Monty (1981). This alignment is due to upward crystal growth by preferential precipitation on the positive hemipyramid {111}. Dark algal micrite filaments are common between and within the prismatic and chevron gypsum crystals (Fig. 8A, B).

Under the microscope, the relations between the algal laminae and the gypsum crystals are varied (Fig. 8C, D). In some cases, the horizontal algal laminations are included in the gypsum crystals without suffering any deformation (Fig. 8C, bottom), or they may form syntaxial growth zones in the gypsum crystals (Fig. 8D). In other cases, they are deformed by crystal growth (Fig. 8C), or may cover discontinuities between crystal growth stages (Fig. 8C). The morphological similarity of the filaments to those described by Rouchy and Monty (1981) from the Messinian gypsum of Cyprus, allowed us to discriminate them from fecal pellets or eggs of organisms. They are very reminiscent of the blue-green algae *Scytonema* as identified by Rouchy and Monty (1981).

The thicker laminae (2 mm–1 cm), that are located between chevron gypsum–algal micrite laminations (Fig. 8A), are composed of reverse-graded gypsum (Fig. 9A) at the central hill outcrop, and of clastic material at the west hill outcrop (Fig. 9B). At the central hill, the reverse-graded laminae consist of fine granular gypsum that fills microtopography between chevron gypsum and is highly enriched in disseminated algal micrite (Fig. 8C). The gypsum crystal size increases upward and is accompanied by the absence of disseminated algal micrite.

In the western hill outcrop, detrital gypsum, quartz and micrite masses enclose and fill microtopography between chevron gypsum crystals (Fig. 8D). They increase in abundance to form whole laminae between chevron gypsum–algal micrite laminae. In the clastic laminae, lenticular and irregular gypsum crystals, which seem to have grown displacively, are seen to be locally replaced by secondary fibrous gypsum crystals (Fig. 9B). The origin of this fibrous gypsum is not fully understood.

The lenticular and irregular gypsum crystals may have been formed as displacively grown crystals following the growth of chevron gypsum and the deposition of the detrital finer gypsum and silt-sized quartz. Thus, the recently formed lenticular and irregular gypsum may be more liable to diagenesis than the older chevron and detrital gypsum? Migration of concentrated brines during later phases of deposition, or due to compaction and dewatering during shallow burial of the evaporite deposits, may have transformed the lenticular and irregular gypsum into hemihydrate or anhydrite pseudomorph. A slight sea-level rise or freshening of the brines, which in turn causes a rise in the water table level within the sabkha, will transform the newly formed hemihydrate or anhydrite into secondary gypsum below the water table. The association of primary chevron gypsum and detrital gypsum crystals with secondary gypsum pseudomorphs of lenticular gypsum crystals is in accordance with the concepts of Warren and Kendall (1985), p. 1021, and Abdel Wahab (1991), p. 9. They showed that a shallow burial of the sabkha sequence would result in the transformation of the primary gypsum into secondary gypsum rather than anhydrite.

Another interesting feature recorded in this facies at the western hill is the occurrence of cylindrical or conical, usually branched, concretion-like structures consisting of rosettes of gypsum around tube-shaped vuggy cores (Fig. 9C). The gypsum crystals that encircle the vugs, form a single crust composed of prismatic and lenticular gypsum crystals that grow displacively within the host clastic material (Fig. 9D).

Fig. 9. Chevron gypsum–algal micrite (cont.). (A) Fine granular gypsum rich in algal micrite disseminations, overlain by clear zones of coarse gypsum crystals that form reverse-graded laminae. Crossed polars; bar = 250 μm. (B) Displacive lenticular gypsum that is pseudomorphically replaced by secondary fibrous gypsum in a matrix of fine detrital quartz and gypsum. Crossed polars; bar = 250 μm. (C) Displacive growth of gypsum rosettes around vugs (probable rootlets). (D) Lenticular arms of the gypsum rosette that are displacively grown in detrital material. Crossed polars; bar = 250 μm. *G* = gypsum, *Alg* = algal micrite, *Q* = quartz.

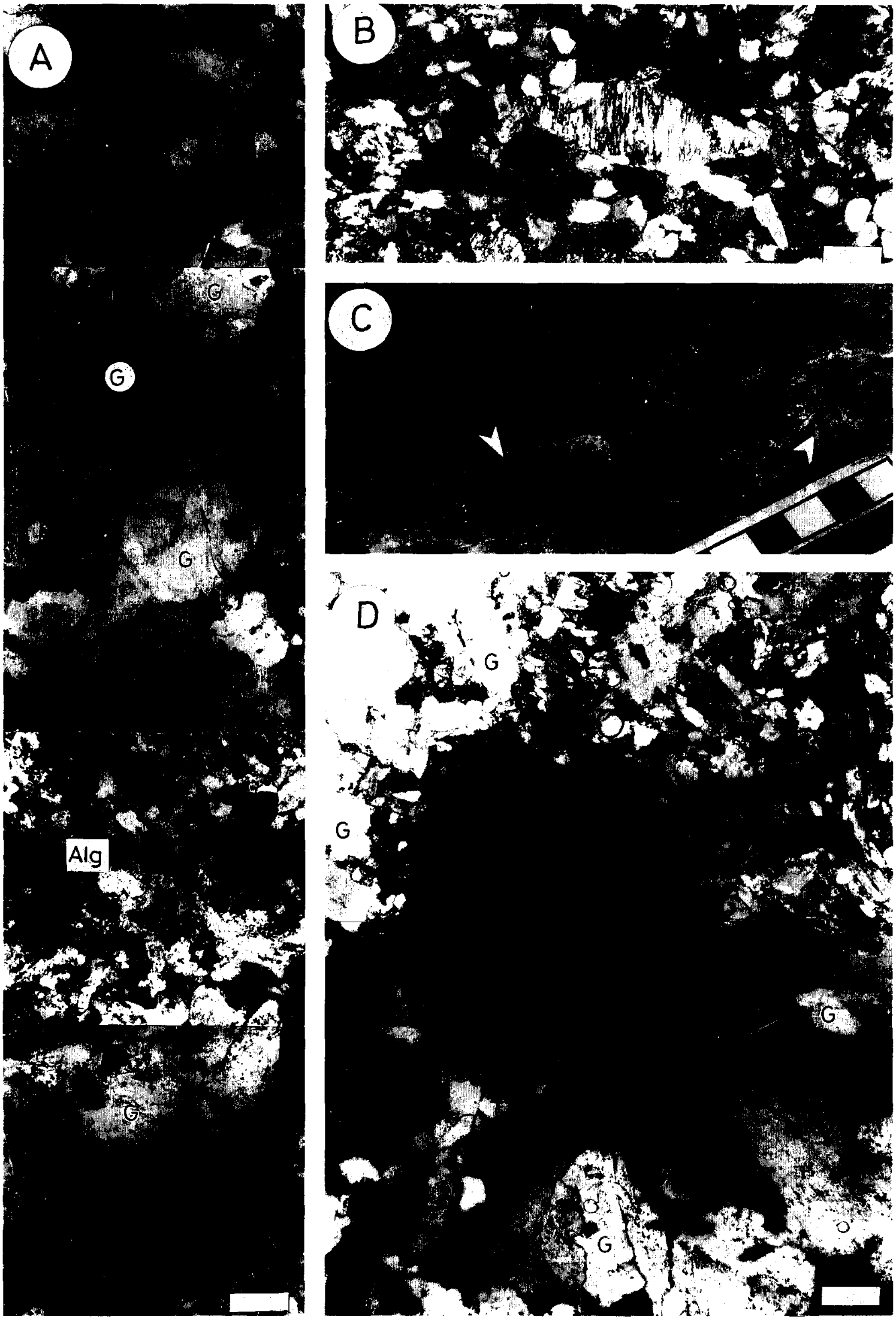
A
G
G
G
Alg
G
B
C
D
G
G
G
G

There is no record of the original material in the vugs, but their elongated and sometimes branched shape, central tube-shaped vugs and the concentric growth of gypsum suggest the former presence of rootlets. These rootlets form the nuclei for displacive growth of gypsum from a saturated brine, with the subsequent decay of the organic core.

The observed gypsum rootlets are 'evaporite rhizoconcretions', similar to root concretions formed by gypsum or anhydrite replacement of plant roots and rhizomes described by Fryberger et al. (1983) and Andreason (1992) from Saudi Arabia and Texas, respectively.

The contortion of the evaporite laminae around the evaporite rhizoconcretions (Fig. 9C), and the scattered nature of the rootlets in this facies, suggest that the rootlets have grown in place and were not washed into the pan. These rootlets record periodic lowering of the water table with subsequent formation of the lenticular gypsum around the rootlets during periodic rising of the water table, and/or evaporative pumping of ground water.

Environment of deposition. The characteristic vertical orientation of elongate and chevron gypsum crystals, their syntaxial overgrowth on the hemipyramid {111}, and the absence of desiccation features suggest subaqueous precipitation of gypsum from concentrated phases of shallow lagoonal waters (Hardie and Eugster, 1971; Schreiber and Kinsman, 1975; Hovorka, 1992; Warren, 1996). Nucleation of the gypsum crystals commenced at the brine–sediment interface and was followed by crystal growth and coalescence of crystal faces until the brine was periodically diluted by fluvial or ground water influxes. The micritic material that encloses and covers the chevron gypsum indicates algal activity during periods of dilution. The absence of marine detrital contaminants within the algal micrite implies no surface connection to normal-marine water but rather a penetration through a barrier (Rouchy and Monty, 1981).

After deposition of prismatic and chevron gypsum at the sediment–brine interface (in the eastern hill outcrop), flooding of marine water to the shallow lagoon took place. This decreased the brine salinities and increased the nucleation density of gypsum crystals promoting numerous fine gypsum crystals that settled over the bottom-grown chevron and prismatic gypsum. Concentration of the brine during gypsum precipitation increases the brine salinity and decreases the nucleation density of gypsum. This promotes fewer but larger gypsum crystals that settled over the finer gypsum forming reverse-graded laminae (Garrison et al., 1978).

The Hutt lagoon, Western Australia, is the modern analog of this depositional environment (Arakel, 1980). In this lagoonal environment, blue-green algal mats cover the pond floor. During summer, as the brine reaches saturation with respect to calcium sulphate, vertically-directed prismatic gypsum develops on the planar surface of the lagoon floor. Ground water influx during the next wet season dilutes pond waters until a new algal mat can develop on top of the gypsum precipitated during the preceding dry season (Arakel, 1980).

The prismatic and chevron gypsum in the western hill outcrop (similar to that recorded from the eastern hill outcrop) probably grew as bottom sediment in a tidal flat environment that was covered with algal mats (Kendall and Skipwith, 1968). This tidal flat environment was subject to deposition of windblown sand, gypsum and micritic limestone from the nearby Miocene formations to the west. These detrital materials filled spaces between the growing gypsum crystals and were entrapped by the growing algal mats.

3.2.3. Wavy algal laminated evaporite facies

This facies forms the top part of the sequence in the study area, in beds ranging in thicknesses from 20 to 40 cm. It consists of regular alternations of anhydrite and lime mud laminae. The anhydrite bands vary in thickness and are contorted. The intercalated lime mud is uneven in thickness, wavy, disrupted, and forms discontinuous bands (Fig. 10A).

Under the microscope, the anhydrite laminae consist of felty epigenetic anhydrite crystals that are replacing former gypsum crystals. Halite crystals are also present in the following forms.

(1) As ghosts of randomly oriented hopper, cubic and triangular halite crystals that are pseudomorphically replaced by gypsum (Fig. 10B). The former halite crystals nucleated at the brine–air interface as hopper crystals which aggregate to form rafts and settle to the bottom. Later, the settled hopper and rafted halite crystals were dissolved by diluted bot-

tom water; this occurred before burial and during the growth of the bottom-nucleated gypsum crystals. This process of early diagenetic replacement of halite by gypsum was not responsible for the apparent slumping of the overlying anhydrite laminae. Similar features of gypsum pseudomorphing single halite crystals were described in the laminated gypsum of Poland (Babel, 1991).

(2) As patches, composed of cube-shaped or rhombohedral halite crystals (probably due to deformation accompanying slumping of the overlying anhydrite laminae) between felted anhydrite. These patches are partially surrounded by algal micrite (Fig. 10C).

(3) As irregular, horizontally aligned halite patches within anhydrite laminae (Fig. 10D). These halite patches are the dissolution residues of former halite laminae. The halite lamina was partially dissolved by upward movement of undersaturated water (probably in a supratidal sabkha setting) prior to lithification of the overlying gypsum. As a result, the gypsum lamina sank and was disrupted to form a nodular-like structure (Fig. 10D). Other parts recombined, or were still connected with the original lamina to form enterolithic-like structures (Fig. 10E). The dissolution of halite crystals created near halite-saturated brines in a zone of active phreatic flow (Warren, 1996) that reprecipitated as efflorescent fibrous crystals in cavities (Fig. 10F), termed 'salt hair' by Rouchy et al. (1994), or may have been released by upward ionic diffusion of NaCl through the unlithified gypsum cover (Ranganthan, 1991).

Environment of deposition. The laminated algal micrite–gypsum–halite facies formed in a marginal-marine salina that occupied a very shallow depression on an arid supratidal flat. In this environment, algal mats grew on the bottom and were accompanied by precipitation of gypsum (now anhydrite) that formed crusts on the algal mats (Fig. 10E). Other gypsum crystals grew displacively as lenticular crystals within the algal mats (Fig. 10G). As long as the mats could obtain water and light, they continued to be viable, but when the salinity became too high, growth ceased (Schreiber et al., 1982). At these higher salinities, crusts of gypsum thickened (Fig. 10E). With further increases in salinity, halite crystallized at the brine–air interface as single hopper crystals that partially aggregated into rafts which settled to form a halite lamina over the gypsum lamina. Also, at this higher salinity range, another species of algae (e.g., *Holobacterium, Dunaleilla*; Cornee et al., 1992) may be favoured. In these mats, displacive halite forms (Fig. 10C) from the supersaturated brine water (Arakel, 1980). After subsequent dilution, gypsum will be precipitated again within the algal mats.

The transformation of gypsum laminae to anhydrite laminae probably took place in a supratidal sabkha setting in the early stage of diagenesis. In this stage, upward movement of undersaturated water caused partial dissolution of the halite crystals (Fig. 10D, E), creating near-surface halite-saturated brines. The highly saline saturated brines became in contact with the gypsum laminae which caused their transformation to anhydrite laminae at much lower temperature (Blount and Dickson, 1973; Shearman, 1985; Hovorka, 1992; Kasprzyk, 1995; Warren, 1996).

3.2.4. Nodular and enterolithic anhydrite facies

This facies makes up the top of the section in the central and western hills outcrops in beds ranging in thickness from 10 to 15 cm. It consists of white to dirty white, spherical to elliptical anhydrite nodules set in a brownish and greenish mudstone matrix (Fig. 11A). Sometimes the nodules coalesce to contorted, ribbon-like, ptygmatic layers of enterolithic anhydrite. Under the microscope, the nodules consist of fine laths of felted epigenetic anhydrite enclosing corroded gypsum relics. The matrix around the anhydrite crystals is composed of detrital silty quartz and clay patches (Fig. 11B) of siliciclastic sediment host.

Environment of deposition. The anhydrite nodules are morphologically and texturally similar to the anhydrite nodules of the modern sabkha of the Arabian Gulf (Kinsman, 1969). Using this modern occurrence as a model, it is believed that the anhydrite nodules formed within subaerially exposed mudstone layers in the capillary fringe just above the ground water table. The supratidal area was probably supplied with ground water through a mechanism similar to the evaporative pumping discussed by Hsü and Siegenthaler (1969). The pore brine was derived from the mixing of lagoonal and continental ground water. Concentration of these ground waters via capillary evaporation caused diagenetic precipi-

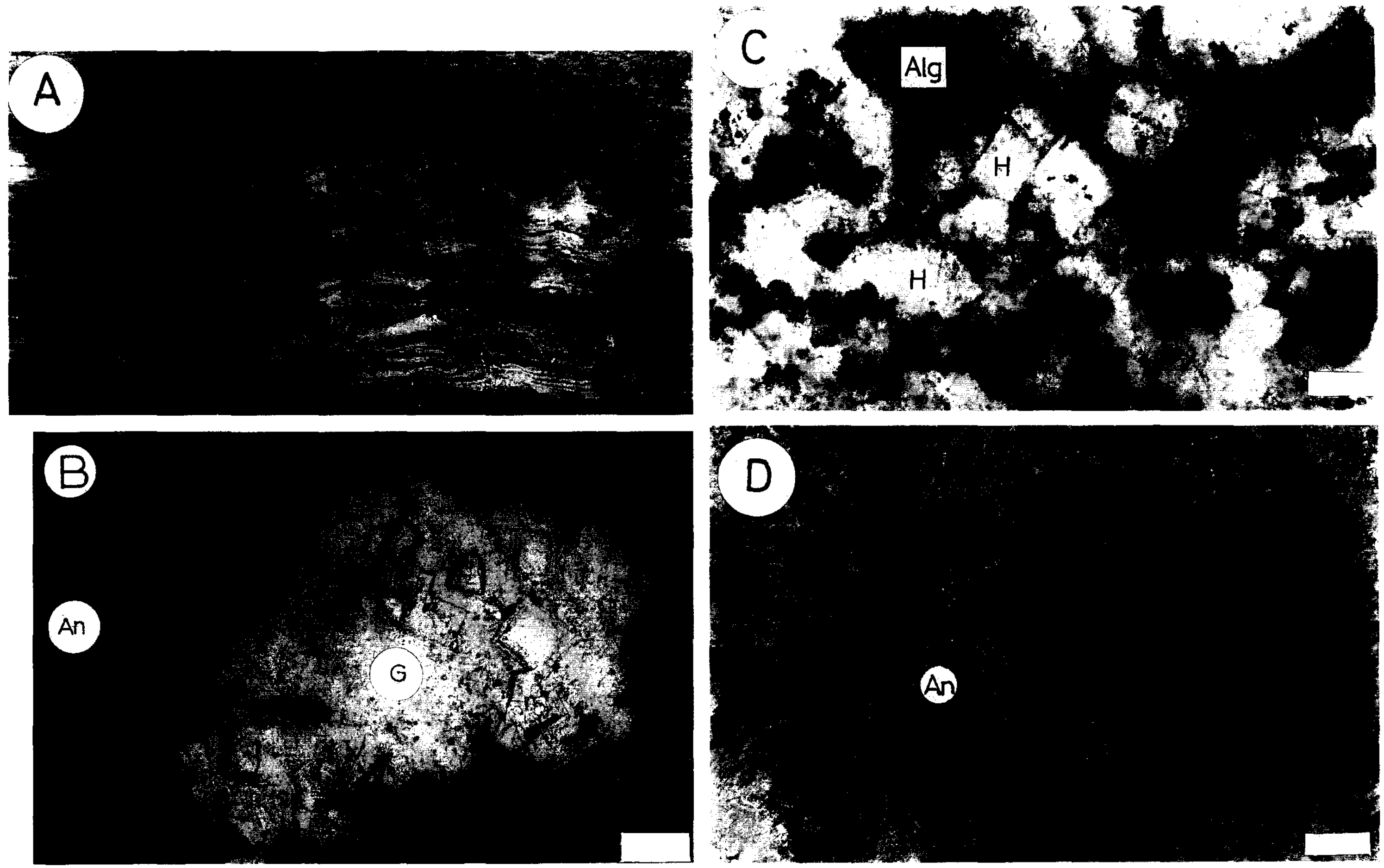

Fig. 10. Wavy algal laminated evaporite facies. (A) Wavy laminated evaporite with some sinks in the mud now filled with evaporite. Note the variable thicknesses of evaporite and clay laminae. (B) Square-shaped and triangular ghosts of former hopper and *rafted halite*, pseudomorphically replaced by gypsum that was partially replaced by felted anhydrite. Crossed polars; bar = 100 μm. (C) Displacive growth of square-shaped and rhombohedron halite in algal micrite. Plane light; bar = 100 μm. (D) Nodular anhydrite formed due to halite dissolution. Crossed polars; bar = 100 μm.

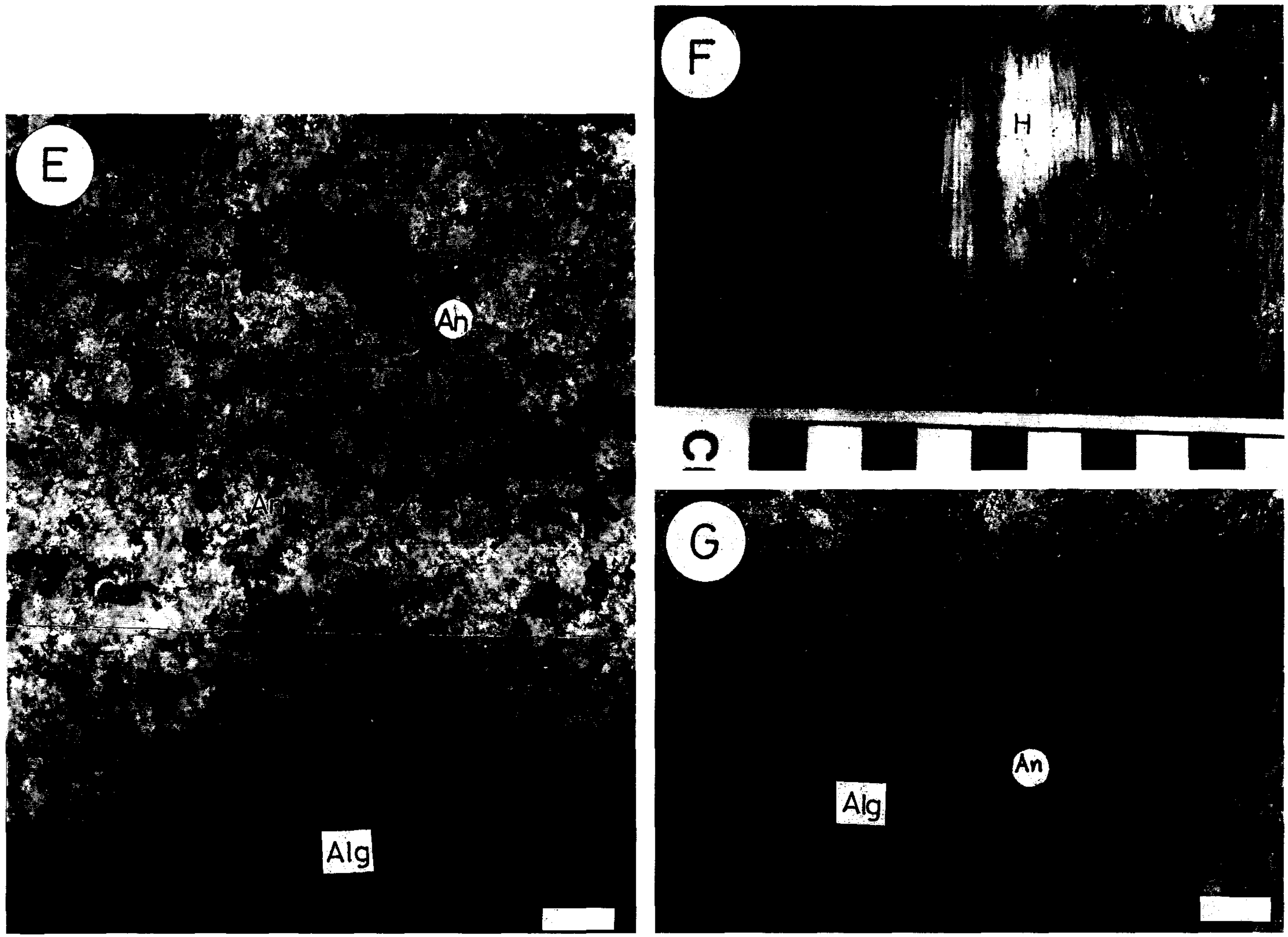

Fig. 10 (continued).(E) Interlamination of algal micrite and anhydrite followed with enterolithic-shaped anhydrite due to salt dissolution. Crossed polars; bar = 250 μm. (F) Fibrous halite crystals (salt hair) fill spaces in gypsiferous mudstone. (G) Lenticular gypsum is pseudomorphically replaced by anhydrite and displacively grown in algal micrite. Crossed polars; bar = 250 μm. G = gypsum, An = anhydrite, Alg = algal micrite, H = halite.

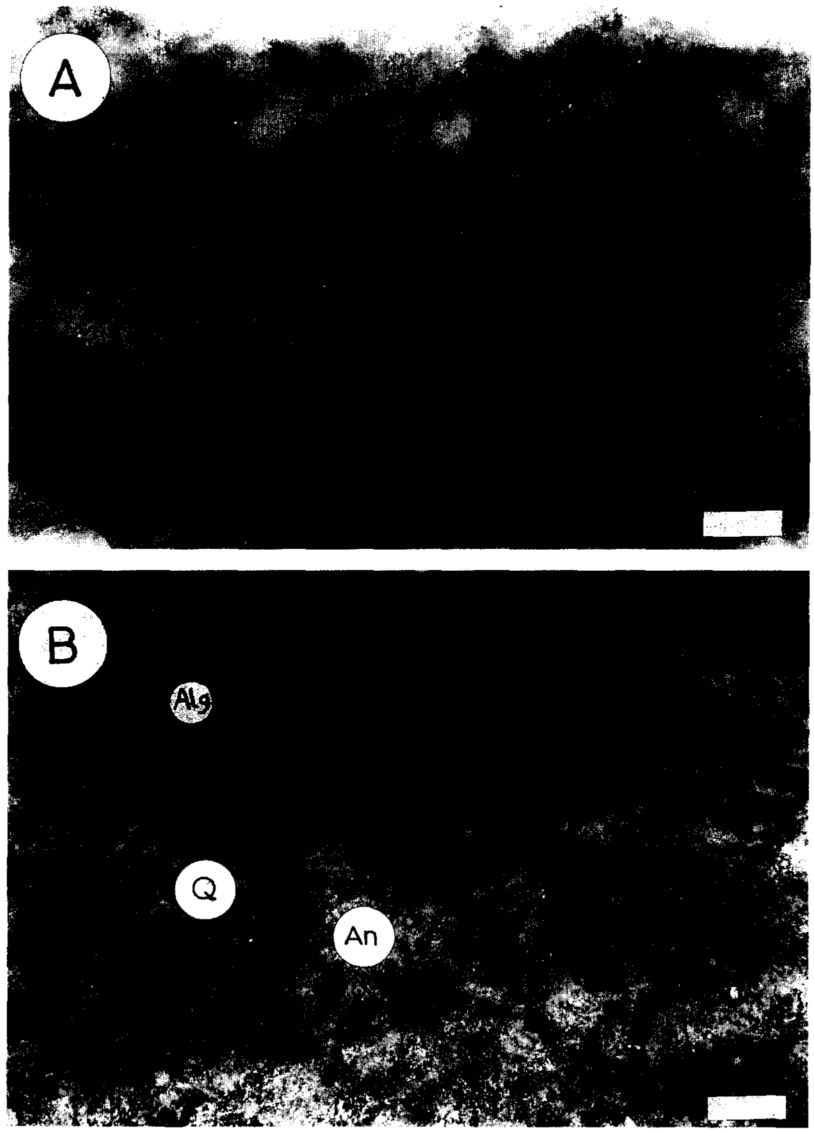

Fig. 11. Nodular to enterolithic anhydrite facies. (A) Polished slab of nodular to enterolithic anhydrite with lime mud in-between. Bar = 2 mm. (B) Felted anhydrite with detrital quartz and clay forming the nodular facies. Crossed polars; bar = 250 μm; *Alg* = algal micrite, *An* = anhydrite, *Q* = quartz.

tation of gypsum within the siliciclastic host. Soon after burial, gypsum (now recorded as fibrous crystals between felted anhydrite) was converted into, or pseudomorphosed by aggregates of anhydrite crystals (Shearman, 1966; Butler, 1970) probably due to the increase in the brine salinity. The pseudomorphs gradually enlarged, lost their crystal shapes, and ultimately grew into anhydrite nodules. Continued growth of anhydrite nodules resulted in closely packed nodules, ultimately in contorted layers and enterolithic folds.

4. Discussion and implications

The Ras Shukeir area is one of the semi-restricted active basins that received continuous evaporite deposition since the Miocene, and Holocene, and also in recent times, indicating intermittent arid episodes over Egypt. The Middle Miocene evaporites were formed in shallow subaqueous to supratidal sabkha–salina complex environments (Aref et al., 1995). The Holocene evaporites share similar facies and characteristics to the older Middle Miocene evaporites and to the younger present-day sabkha–salina complex, which indicates that the Ras Shukeir area has been the marginal platform of evaporite deposition since Miocene time, while the basinal evaporite and those resedimented deeply were located in the central part of the Gulf of Suez (Rouchy et al., 1995).

Most of the Holocene evaporite facies display features characteristic of primary deposition and in situ crystal growth under benthic algal control (e.g., lamination, chevron gypsum). Other evaporite facies are secondary (Warren, 1996), and were diagenetically formed within siliciclastic host sediments (e.g., nodular and enterolithic anhydrite), or have obliterated the original laminated structure [e.g., nodulization (Peryt et al., 1993) of the laminated structure, halite dissolution, etc].

The basal clastic member (pebbly skeletal litharenite facies) was formed in a beach environment and was then cemented by early diagenetic calcite and isopachous dolomite cement. This happened under algal control, in the phreatic zone of a supratidal sabkha environment similar to that recorded by Friedman et al. (1973) from the Red Sea hypersaline pools. Poikilotopic gypsum patches follow the dolomite isopachous cement and were probably formed in the vadose zone. The dissolution of the overlying laminated gypsum layer by meteoric water is the source of the sulphate which was redeposited in the clastic facies.

Restriction of the evaporite depositional environment above the beach sediments probably took place due to uplift of the Quaternary gravely hills which led to the formation of a coastal lagoon (Fig. 12). Water entered this lagoon mainly through seepage as evidenced by the general absence of marine microfauna within the evaporite sequence.

Influxes of marine water of normal salinity into the lagoon led to progressive development of algal mats on the lagoon's bottom. Progressive restriction in circulation and the development of high salinities (by restricted water influx and high evaporation reflux) led to the precipitation of gypsum and halite, mostly in a laminated form (Fig. 12). The laminae are made up of prismatic and granular gypsum that precipitated from the water body, or of chevron gypsum that grew as bottom-nucleated crystals under benthic algal mats. These gypsum laminae are intercalated with algal micrite laminae that formed during periods of dilution. With further increases in salinity, halite hoppers and rafts were formed at the brine–air interface and settled to the bottom to form thin laminae above the gypsum. Sometimes the deposited halite crystals were leached by undersaturated bottom water in the salina during growth of the chevron gypsum.

As the salina became filled with subaqueous evaporites, supratidal sabkha conditions developed and overprinted portions of the subaqueous evaporites. Nodular gypsum displacively grew within the host clastic sediments, then was dehydrated to anhydrite crystals which increased in size and coalesced to form nodular and enterolithic structures. During this stage, alteration of the subaqueous gypsum probably took place. The alteration included: (1) 'nodulization' (Peryt et al., 1993) of the original laminar gypsum; (2) growth and filling of lenticular gypsum in the tubules of possible bioturbation structure similar to that described by Salvany et al. (1994); (3) displacive growth of lenticular gypsum around rootlets; and (4) partial dissolution of the halite laminae by upward-moving undersaturated water, resulting in draping of the gypsum laminae that were dissected to form nodular- and enterolithic-like structures.

The supratidal sabkha condition was also responsible for the development of replacive anhydrite crystals in the Holocene evaporite sequence, similar to those recorded in ancient evaporite sequences. The transformation of gypsum to anhydrite took place close to the surface, where upward movement of fresh water dissolved the halite layers and became oversaturated with respect to halite. These highly saline waters reacted with gypsum crystals at relatively low temperatures and promoted replacement of gypsum by hemihydrate or anhydrite (Rouchy, 1982; Kasprzyk, 1995). The effect of hot, dry climatic conditions in transforming near-surface gypsum to anhydrite in the study area, as suggested by Rouchy et al. (1994), cannot be ruled out.

The Holocene evaporites of the Ras Shukeir area

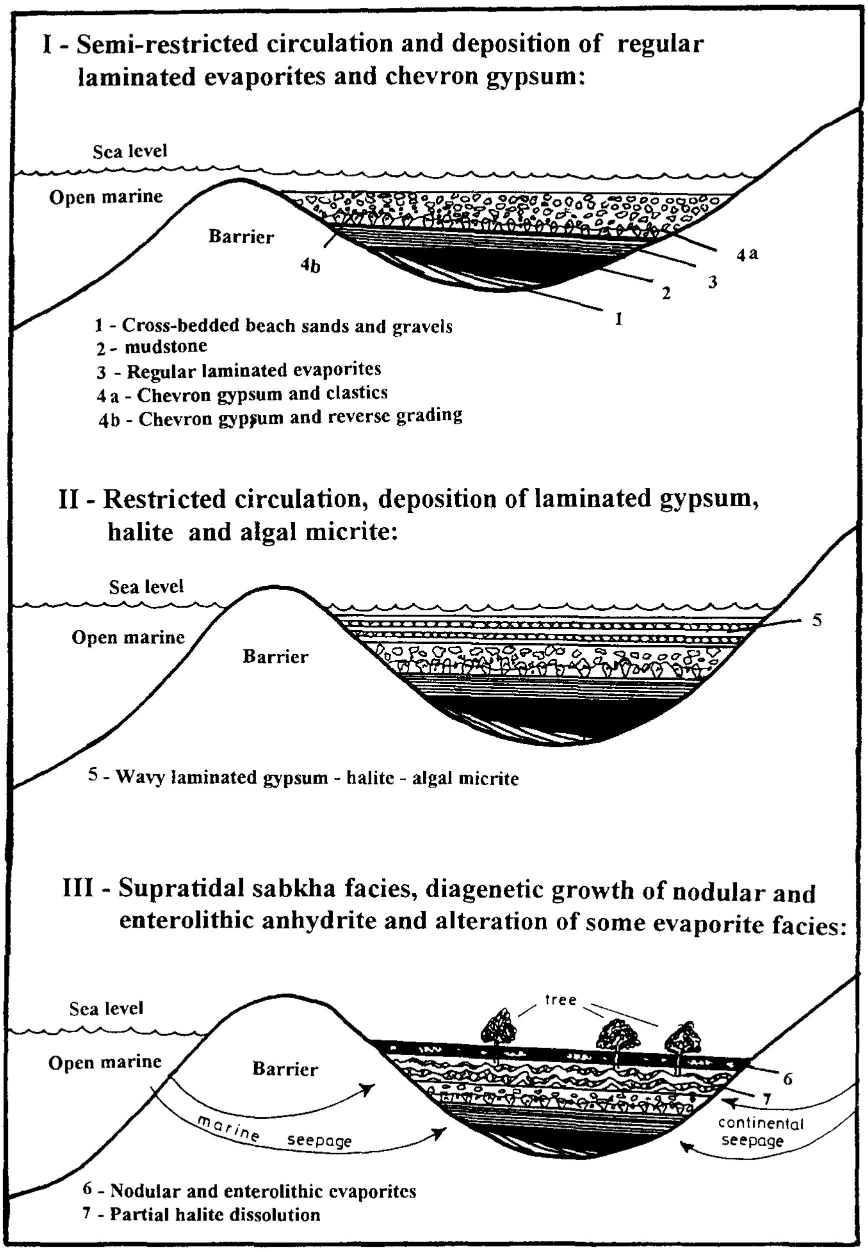

Fig. 12. Depositional model of the evaporite rocks in the Ras Shukeir area.

show sedimentary structures and textures that are similar to those recognized from the Holocene evaporites of the Arabian Gulf, and were most probably formed in a similar depositional environment. The evaporite deposits occur as a seaward-prograding, shoaling-upward sequence over Quaternary gravels. Shallow-water carbonates, associated with the marginal-marine evaporites in the Arabian Gulf (Butler et al., 1982), are not recorded in the Ras Shukeir sequence. A vertical transect in the evaporites of Ras Shukeir is similar to the landward transect in Abu Dhabi sabkha, which begins at the bottom with upper intertidal algal micrite intercalated with laminated gypsum. The gypsum laminae either consist of granular gypsum (lower supratidal environment) or of chevron and prismatic gypsum (subtidal to lower intertidal environment). Alteration of the laminated gypsum to nodular anhydrite probably took place in the middle supratidal environment (Butler et al., 1982). Reworked gypsum and detrital silty quartz were deposited over the landward part of the subtidal to intertidal chevron and prismatic gypsum crystals. In the upper supratidal environment, mixing of marine water and continental ground water from the nearby Quaternary gravely aquifer led to the growth of lenticular gypsum in the presence of terrestrial plants. It also led to the displacive growth of nodular gypsum which was transformed into nodular anhydrite in the vadose zone.

The recorded partial dehydration of the primary gypsum crystals and the alteration of some gypsum–halite structures (e.g., nucleation of lenticular gypsum over rootlets, lenticular gypsum filling tubular structure, 'nodulization' of gypsum laminae, partial halite dissolution and formation of nodular- and enterolithic-like structures) may reflect the action of the nearby continental ground water aquifer in the Quaternary gravels. When the gravels were charged with fresh water, the alteration and dissolution of gypsum and halite took place. On the other hand, during the dry, hot period, deposition of lenticular and nodular gypsum took place; also some gypsum crystals were dehydrated by the residual saline brine.

Acknowledgements

We wish to thank Prof. J.-M. Rouchy, Prof. J. Warren and Prof. G. Philip for their reviews, constructive comments and improvement of our English, which contributed greatly toward clarification of the text.

References

Abdallah, A.M., 1966. Geology of some gypsum deposits in the northern Western Desert of Egypt. Geol. Surv. Egypt., Pap., 41: 1–11.

Abdel Wahab, S., 1991. Ras Shukeir sabkha and associated salina deposits—comparison with a Holocene depositional equivalent. Carbonates Evaporites, 61: 1–12.

Adindani, A.R., Rabjezek, H.A., Youssef, H.A. and Awad, S.M., 1975. Evaluation of El Gharbanyiat gypsum deposits. Ann. Geol. Surv. Egypt, 5: 123–136.

Ahmed, E., Soliman, M. and Essa, M., 1993. Sedimentology and evolution of the Quaternary sediments, NW Red Sea, Egypt. Geol. Soc. Egypt, Spec. Publ., 1: 295–320.

Allen, J.R.L., 1987. Desiccation of mud in the temperate intertidal zone—studies from the Seven Estuary and Eastern England. Philos. Trans. R. Soc. London, Ser. B, 315: 127–156.

Andreason, M.W., 1992. Coastal siliciclastic sabkhas and related evaporative environments of the Permian Yates Formation, north Ward-Estes field, Ward County, Texas. Am. Assoc. Pet. Geol. Bull., 76: 1735–1759.

Arakel, A.V., 1980. Genesis and diagenesis of Holocene evaporitic sediments in Hutt and Leeman lagoons, western Australia. J. Sediment. Petrol., 50/4: 1305–1326.

Aref, M.A.M., Philip, G. and Wali, A.M.A., 1995. Facies and depositional environments of the Miocene evaporites in Shagar area, Gulf of Suez, Egypt. Egypt. J. Geol., 39/2: 835–867.

Astin, T.R. and Rogers, D.A., 1991. Subaqueous shrinkage cracks in the Devonian of Scotland Reinterpreted. J. Sediment. Petrol., 61/5: 850–859.

Babel, M., 1991. Dissolution of halite within the middle Miocene (Badenian) laminated gypsum of southern Poland. Acta Geol. Pol., 41: 165–182.

Blount, C.W. and Dickson, F.W., 1973. Gypsum–anhydrite equilibria in system $CaSO_4$–H_2O and $CaCO_3$–NaCl–H_2O. Am. Mineral., 58: 323–331.

Bosellini, A. and Hardie, L.A., 1973. Depositional theme of marginal marine evaporites. Sedimentology, 20: 5–27.

Butler, G.P., 1970. Holocene gypsum and anhydrite of the Abu Dhabi sabkha, Trucial Coast: an alternative explanation of origin. In: J.L. Rau and L.F. Dellwig (Editors), Third Symposium on Salt, 1, pp. 120–152.

Butler, G.P., Harris, P.M. and Kendall, C.G.St.C., 1982. Recent evaporites from the Abu Dhabi coastal flats. In: Depositional and Diagenetic Spectra of Evaporites. SEPM Core Workshop 3, Calgary, pp. 33–64.

Cody, R.D. and Cody, A.B., 1988. Gypsum nucleation and crystal morphology in analog saline terrestrial environment. J. Sediment. Petrol., 58: 247–255.

Cornee, A., Dickman, M. and Busson, G., 1992. Laminated cyanobacterial mats in sediments of solar salt works—some sedimentological implications. Sedimentology, 39: 599–612.

El Refaeai, A.A.A., 1992. Water resources of southern Sinai, Egypt. Unpubl. Ph.D. Thesis, Cairo University, pp. 357.

Friedman, G.M., Amiel, A.J., Braun, M. and Miller, D.S., 1973. Generation of carbonate particles and laminites in algal mats—example from sea-marginal hypersaline pool, Gulf of Aqaba, Red Sea, Egypt. Am. Assoc. Pet. Geol. Bull., 57: 541–557.

Fryberger, S.G., Al-Sari, A.M. and Clisham, T.J., 1983. Eolian dune, interdune, sandsheet and siliciclastic sabkha sediments of an offshore prograding sand sea, Dhahran area, Saudi Arabia. Am. Assoc. Pet. Geol. Bull., 67: 280–312.

Garrison, R.E., Schreiber, B.C., Bernouilli, D., Fabricius, F.A., Kidd, R.E. and Mélières, F., 1978. Sedimentary petrology and structures of Messinian evaporitic sediments in the Mediterranean Sea, Leg 42A. DSDP, Intl. Rep., 42: 571–612.

Gebelein, C.D. and Hoffman, P., 1971. Algal origin of dolomite in interlaminated limestone–dolomite sedimentary rocks. In: O.P. Bricker (Editor), Carbonate Cements. The John Hopkins Press, Baltimore, pp. 319–326.

Hardie, L.A. and Eugster, P., 1971. The depositional environment of marine evaporites: a case for shallow clastic accumulation. Sedimentology, 16: 187–220.

Hovorka, S.D., 1992. Halite pseudomorphs after gypsum in bedded anhydrite—clue to gypsum anhydrite relationships. J. Sediment. Petrol., 62: 1098–1111.

Hsü, K.J. and Siegenthaler, C., 1969. Preliminary experiments on hydrodynamic movement induced by evaporation and their bearing on dolomite problem. Sedimentology, 12: 11–25.

Hussain, M. and Warren, J.K., 1989. Nodular and enterolithic gypsum: the 'sabkhatization' of Salt Flat playa, west Texas. J. Sediment. Petrol., 64: 13–24.

Kasprzyk, K.A., 1995. Gypsum-to-anhydrite transition in the Miocene of southern Poland. J. Sediment. Res., A65: 348–375.

Keheila, E., Khalifa, H. and El Haddad, A., 1989. Holocene carbonate facies model, Ras Shukeir hypersaline pool and its surrounding sabkha, west Gulf of Suez, Egypt. Sediment. Geol., 63: 155–169.

Kendall, C.G.St.C. and Skipwith, P.A.D.E., 1968. Recent algal mats of a Persian Gulf lagoon. J. Sediment. Petrol., 38: 1040–1058.

Kinsman, D.J.J., 1969. Mode of formation, sedimentary association and diagnostic features of shallow water and supratidal evaporites. Am. Assoc. Pet. Geol. Bull., 53: 830–840.

Kushnir, J., 1981. Formation and early diagenesis of varved evaporite sediments in a coastal hypersaline pool. J. Sediment. Petrol., 51: 1193–1203.

Lowenstein, T.K. and Hardie, L.A., 1985. Criteria for the recognition of salt-pan evaporites. Sedimentology, 32: 627–644.

Maiklem, W.R., Bebout, D.G. and Glaister, R.P., 1969. Classification of anhydrite: a practical approach. Can. Pet. Geol. Bull., 17: 194–233.

Monty, C.L.V., 1986. Microbial dolomites. 12th Int. Sedimentary Congress, Canberra, Australia, pp. 215–216 (Abstr.).

Moore, R.C., 1949. Meaning of facies. Mem. Geol. Soc. Am., 39: 1–34.

Ogniben, L., 1955. Inverse graded bedding in primary gypsum of chemical deposition. J. Sediment. Petrol., 25: 273–281.

Patterson, R.J. and Kinsman, D.J.J., 1982. Formation of diagenetic dolomite in coastal sabkha along the Arabian (Persian) Gulf. Am. Assoc. Pet. Geol. Bull., 66: 28–43.

Peryt, T.M., Orti, F. and Rosell, L., 1993. Sulfate platform–basin transition of the lower Werra anhydrite (Zechstein, upper Permian, western Poland—facies and petrography. J. Sediment. Petrol., 63: 646–658.

Plummer, P.S. and Gostin, V.A., 1981. Shrinkage cracks—desiccation or synaeresis? J. Sediment. Petrol., 51: 1147–1156.

Purser, B.H., 1985. Coastal evaporite systems. In: G.M. Friedman and W.E. Krumbein (Editors), Ecological Studies, 53. Hypersaline Ecosystems. Springer-Verlag, Berlin, pp. 72–102.

Purser, B.H., Soliman, M. and M'Rabet, A., 1987. Carbonate, evaporite, siliciclastic sedimentary transitions in Quaternary rift sediments of the north-western Red Sea. Sediment. Geol., 53: 247–267.

Ranganthan, V., 1991. Salt diffusion in interstitial waters and halite removal from sediments—examples from Red Sea and Illinois basins. Geochim. Cosmochim. Acta, 55: 1615–1625.

Reineck, H.E. and Singh, I.B., 1980. Depositional Sedimentary Environments. Springer-Verlag, Berlin, 549 pp.

Rouchy, J.-M., 1982, La genèse des évaporites Messiniennes de Méditerranée. Muséum National d'Histoire Naturelle, Mémoire, Série C, 50, 267 pp.

Rouchy, J.-M. and Monty, C.L., 1981. Stromatolites and cryptalgal laminites associated with Messinian gypsum of Cyprus. In: C.L. Monty (Editor), Phanerozoic Stromatolites. Springer-Verlag, Berlin, pp. 155–180.

Rouchy, J.-M., Bernet-Rollande, M.C. and Maurin, A.F., 1994. Descriptive petrography of evaporites—applications in the field, subsurface and the laboratory. Evaporite sequences in petroleum exploration, 1. Geological methods. Editions Technip, Paris, pp. 70–123.

Rouchy, J.-M., Pierre, C. and Sommer, F., 1995. Deep-water resedimentation of anhydrite and gypsum deposits in the middle Miocene (Belayim Formation) of the Red Sea, Egypt. Sedimentology, 42: 267–282.

Salvany, J.M., Munoz, A. and Perez, A., 1994. Nonmarine evaporitic sedimentation and associated diagenetic processes of the southwestern margin of the Ebro basin (lower Miocene), Spain. J. Sediment. Petrol., A64: 190–203.

Schreiber, B.C. and Kinsman, D.J.J., 1975. New observations on the Pleistocene evaporites of Montallegro, Sicily and a modern analog. J. Sediment. Petrol., 45: 469–479.

Schreiber, B.C., Roth, M.S. and Helman, M.L., 1982. Recognition of primary facies characteristics of evaporites and the differentiation of these forms from diagenetic over-prints. In: C.R. Handford, R.G. Loucks and G.R. Davies (Editors), Depositional and Diagenetic Spectra of Evaporites: a Core Workshop. SEPM Core Workshop, 3: 1–32.

Sehim, A.A., 1990. Geology and tectonic setting of the Gulf of Aqaba rift. Ph.D. Thesis, Cairo University, 494 pp.

Shearman, D.J., 1966. Origin of marine evaporite by diagenesis. Inst. Min. Metall. Bull., 75: 208–215.

Shearman, D.J., 1985. Syndepositional and late diagenetic alteration of primary gypsum to anhydrite. In: B.C. Schreiber and H.L. Harner (Editors). Sixth International Symposium on Salt Institute, 1, pp. 41–50.

Taher, A.G., 1988. Sedimentology and Geochemistry of the coastal sabkha, Ras Shukeir, Gulf of Suez, Egypt. M.Sc. Thesis, Cairo University, 164 pp.

Wali, A.M.A., 1993. Gharbaniyat stromatolitic gypsum (west Alexandria): a clue from hypersaline syndepositional feature. Bull. Fac. Sci., Zagazig Univ., Egypt, 15/2: 399–422.

Wali, A.M.A., Abdel Wahab, S. and Taher, A.G., 1986. On some supratidal features, Ras Shukeir coastal sabkha, Gulf of Suez. 8th Petroleum Exploration Conference (EGPC), Cairo, 1, pp. 332–343.

Warren, J.K., 1996. Evaporites, brines and base metals: what is an evaporite? Defining the rock matrix. Aust. J. Earth Sci., 43: 115–132.

Warren, J.K. and Kendall, C.G.St.C., 1985. Comparison of sequences formed in marine sabkha (subaerial) and salina (subaqueous) settings: modern and ancient. Am. Assoc. Pet. Geol. Bull., 69: 1013–1023.

White, W.A., 1961. Colloid phenomena in sedimentation of argillaceous sediment. J. Sediment. Petrol., 31: 560–570.